International Journal of Mechatronics and Applied Mechanics
2026, Issue 25, Vol. II

# COMPARATIVE RELIABILITY ASSESSMENT OF A SHAFT–BEARING ASSEMBLY UNDER DIFFERENT DYNAMIC LOADING CONDITIONS

Gergana Tonkova[1], Ventsislav Dimitrov[2], Georgi Tonkov[3], Veselina Dimitrova[2], Sylvester Bozherikov[2], Konstantin Raykov[4], Rumen Yankov[5]
[1]University of Mining and Geology "St. Ivan Rilski", Faculty of Mining Electromechanics, Sofia, Bulgaria
[2]Technical University of Sofia, Faculty of Engineering and Pedagogy Sliven, Department of Mechanics, Mechanical Engineering and Thermal Engineering, Sliven, Bulgaria
[3]Technical University of Sofia, Faculty of Mechanical Engineering, Sofia, Bulgaria
[4]Technical University of Sofia, Faculty of Engineering and Pedagogy Sliven, Department of Electronics, Automation and Information Technologies, Sliven, Bulgaria
[5]College Sliven, Technical University of Sofia, Sliven, Bulgaria
E-mail(s): gtonkova@mgu.bg, vpdd_acad@tu-sofia.bg(✉), gptonkov@tu-sofia.bg, vkdd_acad@tu-sofia.bg, s.bozherikov@tu-sofia.bg, k.raykov@tu-sofia.bg, r.yankov@tu-sofia.bg

**Abstract -** The reliability of laboratory experimental test rigs is an important prerequisite for obtaining accurate, repeatable, and credible experimental results in mechanical engineering. Although extensive research has been conducted on the dynamic behaviour of rotating shafts and rotor systems, the probabilistic reliability assessment of laboratory experimental facilities has received comparatively limited attention. This paper presents a comprehensive methodology for evaluating the reliability of an experimental test rig designed for investigating the bending and torsional vibrations of stepped shafts. The proposed approach is based on classical probabilistic and statistical reliability theory and incorporates the estimation of the probability of failure-free operation, failure probability, failure rate, probability density function, mean time to failure, maintainability, and availability. The methodology also includes statistical processing of the experimental data to evaluate the repeatability and consistency of the obtained results. The obtained results enable a comparative evaluation of the investigated dynamic loading conditions and the identification of operating regimes associated with reduced reliability. The significance of the study lies in the systematic application of established reliability methods to the investigated laboratory shaft–bearing assembly and experimental test rig, providing quantitative support for operational assessment, maintenance planning, and reliability improvement of similar experimental mechanical systems.

**Keywords**: Reliability assessment; Experimental test rig; Probability of failure-free operation; Failure rate; Mean time to failure; Availability; Maintainability; Statistical reliability analysis.

## 1. Introduction

Reliability is one of the fundamental characteristics determining the operational safety, performance, and service life of engineering systems. In rotating machinery, reliability is closely related to dynamic behaviour, vibration characteristics, structural integrity, and the ability of the system to maintain its functional performance throughout its operational life. Consequently, rotor dynamics and vibration analysis have become important research fields in modern mechanical engineering and have been extensively investigated through theoretical, numerical, and experimental studies [1–5].

Particular attention has been devoted to coupled bending–torsional vibrations of rotating shafts because these dynamic phenomena significantly influence the operational behaviour, durability, and reliability of rotor systems. Various analytical, numerical, and experimental approaches have been developed to investigate the dynamic response of rotating shafts under different operating conditions, including cracked rotors, rotor–stator rubbing, geared shaft systems, nonlinear dynamic effects, and frequency modulation phenomena [6–11]. These


dx.doi.org/10.17683/ijomam/issue25/v2.21

studies have considerably advanced the understanding of coupled vibration mechanisms and have provided reliable modelling techniques for modern rotating machinery.

Taken together, the reviewed studies demonstrate that the existing literature is predominantly focused on modelling and characterizing the dynamic response of rotating systems, including vibration mechanisms, structural interactions, and operating-condition effects. While these investigations provide a well-established basis for dynamic analysis, they offer comparatively limited insight into the probabilistic reliability of the experimental facilities used to obtain and validate such results.

The reliability assessment of engineering systems is generally based on probabilistic and statistical methods describing the occurrence and development of failures during operation. Classical reliability theory employs indicators such as the probability of failure-free operation, failure probability, probability density function, failure rate, mean time to failure (MTTF), maintainability, and availability, which constitute the quantitative basis for evaluating the operational reliability of technical systems [12]. In engineering practice, the assessment of rotating machinery is further supported by internationally accepted standards defining the general requirements for vibration evaluation and rotor balancing procedures, thereby ensuring the reliability and consistency of experimental and industrial measurements [13,14].

Although the existing literature provides an extensive theoretical and experimental basis for rotor dynamics and vibration analysis, comparatively limited attention has been devoted to the probabilistic reliability assessment of laboratory test rigs. Most studies focus on the dynamic response of the investigated components, while the reliability of the experimental facility itself is rarely evaluated systematically, despite its direct influence on the repeatability and credibility of experimental results.

The experimental test rig considered in the present study has been progressively developed and improved through a series of previous investigations. Earlier studies examined the bending and torsional vibrations of stepped shafts, evaluated the load-carrying capacity of the experimental stand, determined the natural frequencies of stepped shafts with transition curved sections, and established the theoretical and experimental basis for subsequent investigations [15–18]. These studies provide a comprehensive experimental foundation for performing a probabilistic reliability assessment of the laboratory test rig.

The objective of the present study is to assess the reliability of an experimental test rig using classical probabilistic and statistical reliability indicators under different dynamic loading conditions.

The proposed methodology includes the identification of failure events, estimation of reliability functions, determination of the failure rate, mean time to failure (MTTF), maintainability, and availability, together with a statistical evaluation of the experimental data. The scientific contribution of the present study lies in the systematic application and integration of established probabilistic and statistical reliability methods for the comparative reliability assessment of the investigated laboratory shaft–bearing assembly under different dynamic loading conditions. This application enables the influence of the loading regime on the reliability characteristics of the experimental system to be quantitatively evaluated and provides a structured basis for identifying less favourable operating conditions.

## 2. Materials and Methods

## 2.1 Experimental Test Rig

The experimental investigations were carried out using a laboratory test rig specifically designed for studying the bending and torsional vibrations of stepped shafts under various operating conditions. The test rig enables the investigation of the dynamic behaviour of rotating shafts, determination of their natural frequencies, evaluation of vibration characteristics, and experimental validation of theoretical and numerical rotor-dynamic models.

The mechanical structure of the test rig was designed to provide high structural rigidity and stable operating conditions throughout the experimental programme. Its modular configuration allows the installation of stepped shafts with different geometrical dimensions and structural configurations, thereby extending the applicability of the experimental facility to a wide range of rotor-dynamic investigations.

The main components of the experimental stand include an electric drive with continuously adjustable rotational speed, an elastic coupling, a stepped test shaft, bearing supports, a loading device for applying controlled mechanical loads, and a measuring system for monitoring the dynamic response of the investigated shaft. A general view of the experimental stand is presented in Figure 1, while its structural configuration is illustrated in Figure 2.

The adopted configuration enables controlled variation of the mechanical loading conditions while preserving the basic structural arrangement of the test rig. This feature provides a consistent experimental basis for comparing the response and reliability of the shaft–bearing assembly under different dynamic loading scenarios.

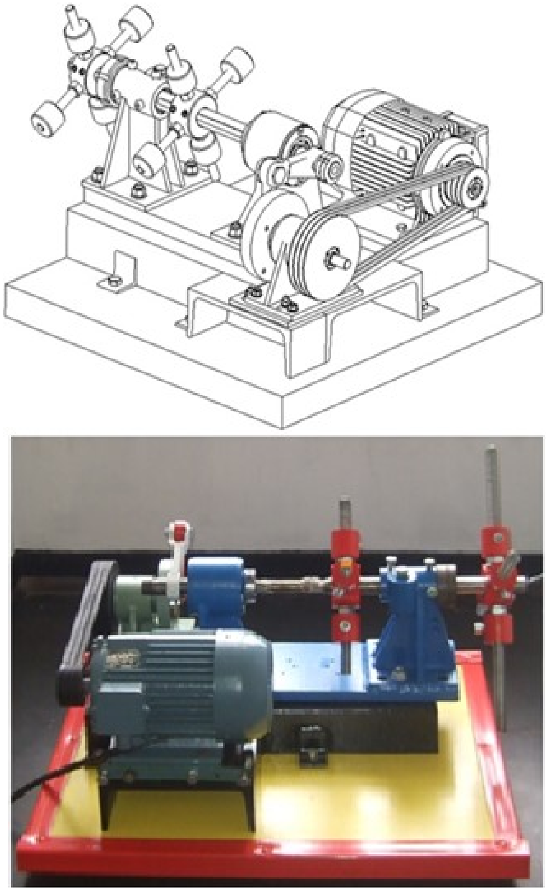

*Figure 1: General view of the experimental test rig [19]*

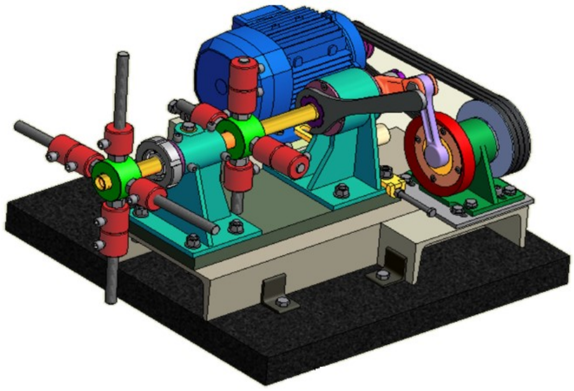

*Figure 2: Structural configuration of the experimental test rig [19]*

The principal technical characteristics of the experimental test rig are summarized in Table 1, including the drive system parameters, the geometric characteristics of the investigated shaft, the bearing assembly, and the main operational parameters used during the experimental investigations.

The mechanical subsystem of the experimental test rig incorporates a kinematic transforming mechanism (KTM), shown in Figure 3, which transmits motion from the electric drive to the tested shaft.

*Table 1. Principal technical characteristics of the experimental test rig [19]*

| Parameter | Specification |
|---|---|
| Test rig type | Modular laboratory test rig |
| Test specimen | Stepped steel shaft |
| Electric motor | Three-phase asynchronous |
| Motor power | 2.2 kW |
| Rotational speed | 1420 $\text{min}^{-1}$ |
| Speed control | Frequency inverter |
| Primary transmission | V-belt drive |
| Secondary transmission | Timing-belt drive |
| Kinematic mechanism | Four-bar linkage with adjustable eccentricity |
| Torque transmission | Intermediate transmission shaft with output flange |
| Shaft support | Rolling bearing supports |
| Loading modes | Continuous rotation and cyclic oscillatory loading |
| Measurement system | Gauges, vibration meter and ADC system |
| Measured quantities | Bending and torsional vibration, dynamic response |

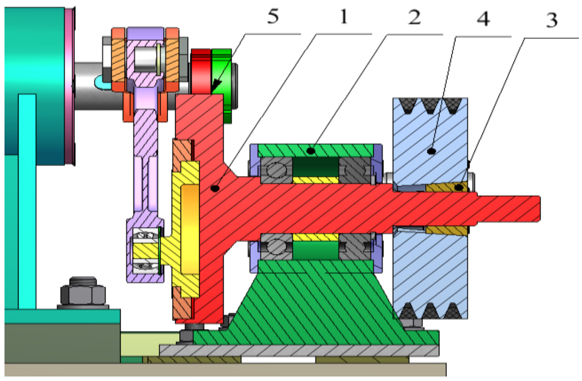


*Figure 3: Kinematic transforming mechanism of the experimental test rig [19]: (1) intermediate transmission shaft; (2) intermediate support assembly; (3) quick-change bushing; (4) interchangeable pulley; (5) output flange.*

The intermediate transmission shaft, mounted in the intermediate support assembly, represents one of the most highly loaded components of the mechanism. It transfers the driving torque through interchangeable transmission systems, including V-belt and timing-belt drives. The input end of the shaft is equipped with a quick-change bushing that enables pulleys of different diameters to be installed, allowing the rotational speed of the tested specimen to be adjusted according to the experimental requirements. The shaft is supported by rolling bearings to ensure stable operation under dynamic loading conditions. At the output end, the transmission shaft is connected to the tested specimen either through a timing-belt transmission or through a four-bar linkage mechanism with adjustable eccentricity. This arrangement enables the generation of both continuous rotational motion and cyclic oscillatory loading, thereby providing flexible operating conditions for the investigation of shaft dynamic behaviour and reliability.

The operating principle of the experimental stand is based on reproducing the actual operating conditions of rotating shafts by continuously controlling the rotational speed while recording the dynamic response of the system. During the experiments, the measured signals are processed using specialized data acquisition equipment, allowing the determination of shaft deformations, vibration characteristics, and stress-related parameters required for the subsequent reliability assessment.

Since the construction, dynamic characteristics, and experimental capabilities of the laboratory stand have already been presented in detail in previous publications and the corresponding doctoral dissertation, only the information necessary for the reliability assessment methodology is included in the present study.

## 2.2 Measurement System

The experimental investigations were carried out using an integrated laboratory measurement system designed to evaluate the dynamic behaviour of the tested shaft under controlled operating conditions. The overall configuration of the experimental setup is presented in Figure 4.

The system comprises a three-phase asynchronous electric motor controlled by a frequency inverter (1), a V-belt transmission (2), a kinematic transforming mechanism (KTM) (3), a flange assembly (4), a four-bar linkage (5), a timing-belt transmission (6), the tested shaft (7), two adjustable loading masses (8 and 9), a supporting frame (10), and a rigid base (11).

The electric motor transmits motion to the kinematic transforming mechanism through the V-belt transmission. Depending on the selected operating configuration, the KTM transfers the motion either through the four-bar linkage or through the timing-belt transmission to the tested shaft.

In the present investigation [15-19], the shaft was operated under reversible oscillatory motion generated by the four-bar linkage, providing representative cyclic loading conditions for the experimental programme.

The tested shaft is supported within the experimental assembly and dynamically loaded by two adjustable masses located between the bearing supports and at the overhung end of the shaft.

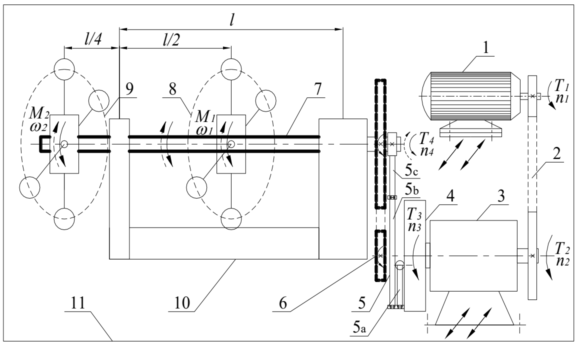


*Figure 4: Kinematic scheme of the tested shaft installed on the experimental test rig [19]: 1 – electric motor;2 – V-belt transmission; 3 – kinematic transforming mechanism (KTM); 4 – flange with shaft supported in the KTM; 5 – four-bar linkage; 6 – timing-belt transmission; 7 – tested shaft;8, 9 – adjustable loading masses; 10 – supporting frame; 11 – base.*

Different loading conditions were obtained by changing the configuration and radial position of the adjustable masses, while the oscillation angle was controlled through the eccentricity of the four-bar linkage. The rotational speed was continuously regulated by the frequency inverter, enabling a wide range of operating conditions.

The adopted experimental system provides stable and repeatable operating conditions, allowing systematic investigation of the shaft response under different combinations of rotational speed, oscillation angle, and loading configuration. The experimental data obtained from this setup constitute the basis for the reliability assessment methodology presented in the following sections.

## 2.3 Experimental Procedure

The experimental programme was designed to investigate the reliability of the tested shaft under different dynamic loading conditions. The operating conditions were varied by modifying the configuration of the adjustable loading masses, the oscillation angle, and the rotational speed of the driving system. These parameters enabled the simulation of representative service conditions while maintaining identical shaft geometry throughout all experiments.

The shaft was driven under reversible oscillatory motion generated by the four-bar linkage mechanism. The oscillation angle was adjusted by changing the eccentricity of the mechanism, whereas the rotational speed was continuously regulated by the frequency inverter. Two operating regimes of the kinematic transforming mechanism (KTM) were considered, producing the corresponding dynamic loading conditions for the tested shaft.

To evaluate the influence of the loading configuration on the shaft behaviour, six loading arrangements were investigated. The experimental cases differed in the number, position and geometric configuration of the adjustable masses mounted on the shaft. For each loading arrangement, the same shaft geometry and experimental procedure were maintained, while only the loading configuration was modified. The investigated loading cases are summarised in Table 2.

*Table 2. Experimental loading configurations used in the investigation [19]*

| Case | Loading configuration | Mass arrangement |
|---|---|---|
| 1 | One loading mass positioned between the bearing supports | Four equally spaced masses symmetrically distributed on the four arms |
| 2 | One loading mass mounted at the overhung end | Four equally spaced masses symmetrically distributed - four arms |
| 3 | One loading mass positioned between the bearing supports | Two adjacent arms equipped with two masses each, while the remaining arms were unloaded |
| 4 | One loading mass mounted at the overhung end of the shaft | Same asymmetric configuration as Case 3 |
| 5 | Two loading masses: one between the bearing supports and one at the overhung end | Both loading masses equipped with four symmetrically distributed masses |
| 6 | Two loading masses: one between the bearing supports and one at the overhung end | Both loading masses equipped with asymmetric mass distributions arranged in opposite orientations |

Experimental loading configurations adopted for the investigated shaft. The principal experimental parameters adopted throughout the investigation are presented in Table 3. The loading programme consisted of six loading configurations evaluated under two operating regimes, resulting in a total of twelve investigated cases.

Principal operating parameters used during the experimental investigation. For each loading case, the shaft was subjected to the same experimental procedure, while only the loading configuration was modified. The measured responses obtained from the twelve investigated cases were subsequently processed to determine the stress–strain state of the shaft and to perform the reliability assessment presented in the following sections.

This experimental design provided a consistent basis for the subsequent analytical and numerical processing and comparative reliability assessment of the investigated operating conditions.

*Table 3. Principal experimental parameters used in the investigation [19].*

| Parameter | Symbol | Value |
|---|---|---|
| Central loading assembly | $G_1$ | 57 N |
| Overhung loading assembly | $G_2$ | 65 N |
| Radius of loading configurat.1 | $R_1$ | 0.135 m |
| Radius of loading configurat. 2 | $R_2$ | 0.110 m |
| Rotational speed of the kinematic transforming mechanism | n | 673 $\min^{-1}$ |
| Angular velocity | ω | 70.5 $s^{-1}$ |
| Number of loading configurations | – | 6 |
| Number of operating regimes | – | 2 |
| Total investigated cases | – | 12 |

## 2.4 Data Processing

The experimental data obtained from the investigated loading cases were processed using a combined experimental, analytical and numerical approach. The measured operating parameters were first verified and transformed into the input quantities required for the numerical evaluation of the shaft behaviour. These quantities included the loading configuration, rotational speed, oscillation angle, loading forces and the geometric characteristics of the loading assemblies.

Based on the experimentally established operating conditions, analytical calculations were performed to determine the force and kinematic parameters acting on the shaft. The analytical procedure provided the loading forces, inertial effects, reaction forces, bending moments, shear forces and torsional moments, which served as the input data for the subsequent numerical analysis.

The numerical evaluation of the shaft was carried out using the MITCalc engineering software. The computational model incorporated the experimentally defined shaft geometry, material properties, bearing arrangement, loading positions and dynamic loading conditions. Based on the analytical input parameters, the software automatically calculated the mechanical response of the shaft under each investigated loading configuration.

The calculated results included support reactions, shaft deflection, angle of twist, bending moments, shear forces, equivalent (von Mises) stresses, and the corresponding static and dynamic safety factors. These quantities were subsequently analysed to identify the most highly stressed regions of the shaft and to evaluate the influence of the loading configuration on its mechanical behaviour.

The complete workflow adopted for the processing of the experimental and numerical data is presented in Figure 5. The proposed methodology integrates the experimental investigation, analytical calculations and numerical modelling into a unified data-processing framework. The resulting stress–strain characteristics obtained through this procedure constitute the input data for the reliability assessment methodology presented in the following section.

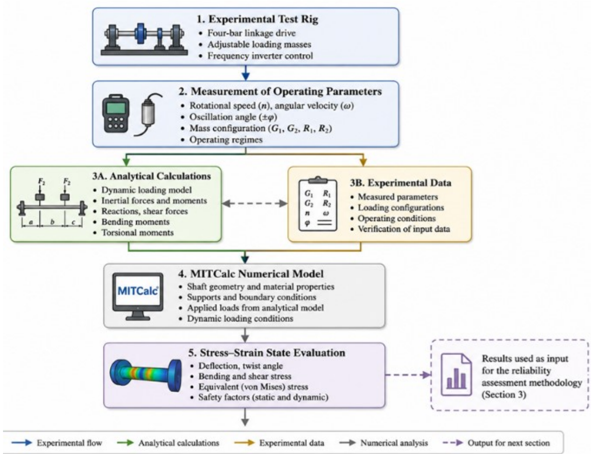


*Figure 5: Integrated workflow of the experimental, analytical and numerical data-processing methodology adopted in the present study.*

The described procedure ensured consistent processing of all twelve investigated loading cases and established a common basis for the comparative evaluation of the shaft behaviour under different dynamic loading conditions. The processed stress–strain data obtained from this workflow were subsequently employed in the reliability assessment methodology described in Section 3.

## 3. Reliability Assessment Methodology

### 3.1 Reliability Assessment Concept

The safe operation of rotating shafts subjected to dynamic loading depends not only on their static strength but also on the combined influence of loading configuration, stress distribution, structural deformation and operating conditions. Conventional shaft design is generally based on static or dynamic safety factors, which provide valuable information regarding the mechanical resistance of the structure. However, these quantities alone do not fully describe the overall operational reliability of shafts operating under variable bending and torsional loading conditions.

In the present study, a comprehensive reliability assessment methodology is proposed by integrating the experimental measurements, analytical calculations and numerical simulations described in Section 2. The developed methodology combines the experimentally established operating conditions with the calculated stress–strain response of the shaft in order to evaluate its reliability under different loading configurations.

Unlike conventional approaches based solely on a single mechanical parameter, the proposed methodology considers multiple reliability-related indicators describing the mechanical behaviour of the shaft. These indicators are evaluated simultaneously and subsequently combined into a single integrated reliability measure, allowing a comparative assessment of different operating conditions and loading configurations.

The proposed methodology is intended to provide a systematic engineering tool for identifying the loading conditions that most significantly affect the mechanical reliability of dynamically loaded shafts. The overall assessment procedure is presented in the following subsections.

### 3.2 Fundamental Mathematical Relationships for Reliability Assessment

The mathematical formulation adopted in this study is based on the fundamental relationships of classical reliability theory. These relationships are presented explicitly to define the probabilistic quantities, modelling assumptions, and calculation sequence subsequently applied to the investigated shaft–bearing assembly and experimental test rig.

The quantitative reliability assessment of the investigated shaft is based on the relationships between the probability of failure-free operation, the probability density of failures, the failure intensity and the availability coefficient. These indicators describe different but mutually related aspects of the operational behaviour of the shaft. The probability of failure-free operation characterises its ability to remain operational during a specified period, whereas the failure intensity and failure density describe the temporal occurrence of failures. For a recoverable system, the availability coefficient additionally accounts for the time required to restore the system after a failure.

The probability of failure-free operation is defined as the probability that the operating time T to the first failure exceeds a specified operating time t:

$$P(t) = P\{T > t\} \tag{1}$$

Accordingly, *P(t)* is a non-increasing function satisfying the conditions

$$P(0) = 1, \qquad \lim_{t \to \infty} P(t) = 0 \tag{2}$$

The general relationship between the probability of failure-free operation and the time-dependent failure intensity is expressed by the fundamental reliability equation

$$P(t) = \exp\left[-\int_0^t \lambda(\tau)\, d\tau\right] \tag{3}$$

where:

-P(t) is the probability of failure-free operation during the interval [0,t];

-$\lambda(\tau)$ is the failure-intensity function;
-$\tau$ is the integration variable representing operating time.

Equation (3), corresponding to the fundamental relationship presented in the adopted reliability methodology, allows the failure intensity to vary over the operating period. Therefore, it may be applied not only to a constant-rate failure process but also to systems whose failure behaviour changes due to wear, fatigue accumulation, deterioration of supports or variations in dynamic loading.

The failure intensity can be obtained from the reliability function by rearranging Eq. (3):

$$\lambda(t) = -\frac{d}{dt}\ln P(t) \qquad (4)$$

Equivalently,

$$\lambda(t) = -\frac{1}{P(t)}\frac{dP(t)}{dt} \qquad (5)$$

The failure intensity represents the conditional rate of failure at time ttt, provided that the shaft has remained operational up to that time. It should therefore not be interpreted merely as the number of failures per unit time. It describes the tendency of an operating shaft to fail within the following infinitesimal time interval.

The reliability methodology distinguishes the probability of failure-free operation, failure density and failure intensity as the principal indicators of the failure-free behaviour of a technical object.

For the normal operating period, during which no pronounced ageing trend is assumed, the failure intensity may be approximated as constant:

$$\lambda(t) = \lambda_0 = \text{const} \qquad (6)$$

Substitution of Eq. (6) into Eq. (3) gives:

$$P(t) = \exp\left[-\int_0^t \lambda_0 \, d\tau\right] \qquad (7)$$

and therefore:

$$P(t) = e^{-\lambda_0 t} \qquad (8)$$

Equation (8) represents the exponential reliability law. Within the present methodology, it is used as the initial analytical model for assessing the probability that the investigated shaft will remain operational over a prescribed operating period.

When the probability P(t) is known for a particular operating time, the constant failure intensity may be determined inversely as

$$\lambda_0 = -\frac{\ln P(t)}{t} \qquad (9)$$

This inverse relationship is particularly useful when the available information consists of an experimentally established or prescribed reliability level at a given operating time. Such an approach is demonstrated in Example 4 of the source methodology, where the failure intensity is determined from a given probability of failure-free operation and subsequently used to predict reliability over longer operating periods.

The probability of failure Q(t) is complementary to the probability of failure-free operation:

$$Q(t) = 1 - P(t) \qquad (10)$$

Although *Q(t)* will be considered in greater detail in Section 3.3, it is introduced here because it provides the basis for defining the failure probability density.

The probability density of failures is determined by:

$$f(t) = \frac{dQ(t)}{dt} \qquad (11)$$

Considering Eq. (10), the same quantity may be written as:

$$f(t) = -\frac{dP(t)}{dt} \qquad (12)$$

The failure density *f(t)* describes the distribution of failures over the operating time. Unlike *λ(t)*, which is conditional on survival up to time *t*, *f(t)* describes the unconditional probability of failure per unit time. The relationship between failure density, failure intensity and reliability is:

$$f(t) = \lambda(t)P(t) \qquad (13)$$

Consequently,

$$\lambda(t) = \frac{f(t)}{P(t)} \qquad (14)$$

For the exponential reliability model, substitution of Eqs. (6) and (8) into Eq. (13) gives:

$$f(t) = \lambda_0 e^{-\lambda_0 t} \qquad (15)$$

Thus, under the assumption of a constant failure intensity, the failure density decreases exponentially with operating time, while the conditional failure intensity remains constant.

The distinction between *f(t)* and *λ(t)* is important:

$$f(t) \neq \lambda(t) \qquad (16)$$

except at the initial instant when *P(0)=1*. Their relationship is always governed by Eq. (13).

In the context of the investigated shaft:

- P(t) represents the probability that the shaft remains operational during the prescribed operating period;

- Q(t) represents the probability that a failure occurs before the end of this period;
- f(t) describes how failures are distributed over operating time;
- λ(t) characterises the conditional failure tendency of a shaft that has remained operational up to time *t*.

The calculation sequence involving *P(t)*, *Q(t)*, *f(t)* and the mean failure-free operating time is illustrated in Example 3 of the adopted methodology. However, in the present study, the corresponding relationships are applied to the dynamically loaded shaft rather than to the mechanical system considered in that example.

Because the investigated shaft and the experimental test rig are recoverable technical systems, their operational assessment should not be restricted to failure-free operation alone. After a failure, the system may be inspected, repaired, adjusted or restored to an operational state. It is therefore necessary to account for both the failure process and the recovery process.

For an object that alternates between an operational state and a failed state, the stationary availability coefficient is defined as:

$$K_A = \frac{T_0}{T_0 + T_R} \tag{17}$$

where:
- $K_A$ is the stationary availability coefficient;
- $T_0$ is the mean failure-free operating time or mean time between failures, depending on the type of object considered;
- $T_R$ is the mean recovery time.

The source methodology defines the availability coefficient as the probability that, after a sufficiently long operating period, the object is found in an operational state at an arbitrarily selected moment.

For the exponential reliability law,

$$T_0 = \frac{1}{\lambda_0} \tag{18}$$

If the recovery process is also described by an exponential distribution, the mean recovery time is:

$$T_R = \frac{1}{\mu} \tag{19}$$

where $\mu$ is the recovery intensity.

Substitution of Eqs. (18) and (19) into Eq. (17) yields:

$$K_A = \frac{\frac{1}{\lambda_0}}{\frac{1}{\lambda_0} + \frac{1}{\mu}} \tag{20}$$

or, after simplification,

$$K_A = \frac{\mu}{\lambda_0 + \mu} \tag{21}$$

An equivalent expression is:

$$K_A = \frac{1}{1 + \lambda_0 T_R} \tag{22}$$

The corresponding unavailability coefficient is:

$$K_U = 1 - K_A \tag{23}$$

and therefore:

$$K_U = \frac{T_R}{T_0 + T_R} = \frac{\lambda_0}{\lambda_0 + \mu} \tag{24}$$

The stationary availability coefficient simultaneously accounts for two operational characteristics:
- the frequency with which failures occur, represented by $\lambda_0$ or $T_0$;
- the time required to restore the system, represented by $T_R$ or μ.

A high probability of failure-free operation does not necessarily ensure high availability if the corresponding recovery time is excessively long. Conversely, a system with a comparatively higher failure intensity may still exhibit acceptable availability when failures are detected and repaired rapidly.

The source methodology applies this approach in Example 6, where the stationary and instantaneous availability coefficients are determined from the failure intensity and the mean recovery time. The same calculation principle is adopted in the present study, but the reliability and recovery parameters are related to the investigated shaft and its associated test system.

The initial conditions under which the availability model is formulated are the following:
- the system may occupy either an operational or a failed state;
- operating and recovery intervals alternate consecutively;
- the initial model concerns a single object without redundancy;
- the failure process is initially represented by an exponential distribution;
- the recovery process is also represented by an exponential distribution.

These assumptions correspond to the formulation of the availability indicators in the adopted methodology.

The mathematical sequence used in the present reliability assessment can therefore be summarised as:

$$\lambda(t) \to P(t) \to Q(t) \to f(t) \to T_0 \to K_A \tag{25}$$

However, only the fundamental relationships for *P(t)*, *λ(t)*, *f(t)* and *KA* are established in the present subsection. The operating-time indicators, failure and recovery times, failure probability, failure flow and recovery flow are defined and evaluated separately in Section 3.3.

## 3.3 Reliability and Recoverability Indicators

The mathematical relationships presented in the previous subsection constitute the theoretical basis for the reliability assessment of the investigated shaft. However, the practical evaluation of the experimental results requires a set of quantitative indicators that describe different aspects of the operational behaviour of the shaft and the experimental test system [12].

For recoverable mechanical systems, reliability assessment cannot be based solely on the probability of failure-free operation. It is also necessary to evaluate the expected operating time before failure, the recovery process, the availability of the system and the statistical characteristics of failure occurrence. Therefore, the present methodology employs the principal reliability and recoverability indicators adopted in classical reliability theory and applies them to the dynamically loaded shaft investigated in this study.

The indicators considered in the present work include:

- mean time to failure (MTTF) or mean time between failures (MTBF), depending on the adopted reliability model;
- mean recovery time (MTTR);
- probability of failure-free operation;
- probability of failure;
- failure intensity;
- failure density;
- failure flow;
- recovery flow;
- availability coefficient.

Together, these quantities provide a comprehensive description of the operational reliability of the investigated shaft under cyclic dynamic loading.

The mean time to failure represents the expected operating time until the first failure of a non-repairable object. It is defined as:

$$MTBF = \int_0^\infty P(t)dt \tag{26}$$

For the exponential reliability model,

$$MTBF = \frac{1}{\lambda} \tag{27}$$

The investigated shaft operates under repeated loading and may be repaired or replaced after failure. Consequently, the mean operating time between two consecutive failures is a more representative indicator than the time to the first failure.

For recoverable systems, the principal time indicator is the mean time between failures (MTBF). It is determined by:

$$MTBF = \frac{1}{m}\sum_{i=1}^{m} T_i \tag{28}$$

where

- $T_i$ is the operating time between two consecutive failures;
- m is the number of observed failures.

This indicator characterises the operational durability of the investigated shaft and forms one of the principal quantities used for calculating the availability coefficient.

After the occurrence of a failure, the shaft or the experimental system is restored to an operational state by inspection, adjustment or replacement of damaged components.

The mean repair time is:

$$MTTR = \frac{1}{n}\sum_{i=1}^{n} T_{Ri} \tag{29}$$

where

-$T_{Ri}$ is the repair duration after the iii-th failure;

-n is the number of repairs.

A reduction of MTTR increases the operational availability of the investigated system even if the failure frequency remains unchanged.

The probability that the shaft remains operational throughout the prescribed operating interval is:

$$P(t) = e^{-\lambda t} \tag{30}$$

This quantity represents one of the most important reliability indicators because it directly evaluates the likelihood that the shaft performs its intended function without interruption.

The complementary probability of failure is

$$Q(t) = 1 - P(t) \tag{31}$$

Unlike the probability of failure-free operation, this quantity characterises the cumulative probability that a failure occurs before the specified operating time.

For recoverable systems, failures occur repeatedly during operation.

The failure flow represents the stochastic process describing the occurrence of consecutive failures in time.

For stationary operating conditions,

$$\omega(t) = \lambda \tag{32}$$

The failure flow therefore characterises the average frequency of failures occurring during continuous operation of the investigated shaft.

Following each failure, the shaft is restored to operational condition.

The recovery flow is characterised by the recovery intensity:

$$\mu = \frac{1}{MTTR} \tag{33}$$

This indicator describes the average capability of the maintenance process to restore the investigated shaft to service.

The operational availability combines both the reliability and the maintainability of the investigated shaft.

It is determined by:

$$K_A = \frac{MTBF}{MTBF + MTTR} \tag{34}$$

The availability coefficient expresses the probability that the shaft is in an operational condition at an arbitrary instant during long-term operation. Consequently, high availability may be achieved either by increasing the operating time between failures or by reducing the repair time after each failure.

The indicators introduced above are mutually dependent and collectively describe the operational behaviour of the investigated shaft.

The probability of failure-free operation determines the probability of failure, which in turn defines the failure density and the failure intensity. These quantities determine the mean operating time between failures, while the repair duration characterises the recovery process. Finally, the combined influence of MTBF and MTTR determines the availability coefficient, which represents the principal operational indicator used in the present investigation.

Accordingly, the logical sequence of the adopted reliability assessment methodology may be summarised as:

$$P(t) \rightarrow Q(t) \rightarrow f(t) \rightarrow \lambda \rightarrow MTBF \rightarrow MTTR \rightarrow K_A$$

The indicators introduced in this subsection constitute the basis for the reliability assessment procedure presented in the following section.

## 3.4 Reliability Assessment Procedure

The reliability assessment methodology proposed in the present study integrates analytical reliability theory, experimental measurements and numerical simulations into a unified evaluation procedure. Unlike conventional approaches that rely solely on statistical failure data, the adopted methodology combines experimentally measured dynamic loading with analytical reliability indicators in order to evaluate the operational behaviour of the investigated shaft.

The assessment procedure follows a sequential workflow in which each reliability indicator is determined from the previously established mathematical relationships. Initially, the operating conditions of the investigated shaft are identified through the experimental programme described in Section 2. The measured loading conditions, rotational speed and deformation response are subsequently introduced into the analytical reliability model developed in Sections 3.2 and 3.3.

The reliability evaluation procedure consists of the following principal stages:

- Definition of the investigated mechanical system and its operating conditions.
- Identification of the loading regime and failure criteria.
- Determination of the probability of failure-free operation.
- Evaluation of the probability of failure.
- Determination of the failure density and failure intensity.
- Calculation of the mean operating time between failures.
- Estimation of the recovery characteristics.
- Determination of the operational availability.
- Overall reliability assessment of the investigated shaft.

The adopted procedure enables each reliability indicator to be evaluated independently while preserving the mathematical relationship between the individual quantities. Consequently, the complete reliability behaviour of the investigated shaft can be assessed using a unified methodology.

The combination of experimental measurements, analytical reliability relationships and engineering interpretation provides a comprehensive framework for evaluating dynamically loaded rotating shafts subjected to cyclic operating conditions.

## 4. Reliability Results and Discussion

Three operating scenarios were considered to evaluate the influence of the dynamic loading conditions on the reliability of the shaft–bearing assembly:

1. Symmetric constant dynamic loading;
2. Variable dynamic loading with intermittent overloads;
3. Asymmetric constant dynamic loading.

For each scenario, N=20 shaft–bearing assemblies were considered over an individual observation period of $t_{test}$=100 h. Thus, the total accumulated operating time for each loading regime was:

$$T_{\Sigma} = Nt_{test} = 20 \times 100 = 2000\ h \tag{35}$$

A failure was registered when the vibration level, shaft runout, or bearing temperature exceeded the prescribed allowable limit, or when damage to the shaft support required shutdown and corrective maintenance. The operating conditions and the assumed failure and restoration data are summarised in Table 4.

*Table 4. Input data for the reliability assessment*

| Parameter | Symmetric constant loading | Variable loading with intermittent overloads | Asymmetric constant loading |
|---|---|---|---|
| Rotational speed *n, min⁻¹* | 1450 | 1450 | 1450 |
| Nominal torque *M, N·m* | 180 | 180 | 180 |
| Max. torque $M_{max}$, *N·m* | 180 | 270 | 180 |
| Radial force $F_r$, kN | 1.20 | 1.40 | 1.80 |
| Eccentricity *e, mm* | <0.10 | 0.40 | 0.80 |
| Number of tested assemblies | 20 | 20 | 20 |
| Total accumulated operating time | 2000 | 2000 | 2000 |
| Number of failures | 3 | 5 | 7 |
| Total restoration time, *h* | 18 | 35 | 49 |

For the symmetric constant-loading scenario, the failure rate was calculated as (14):

$$\lambda_1 = -\frac{\ln P(t)}{t} = \frac{r_1}{T_{\Sigma,i}} = \frac{3}{2000} = 1.50 \times 10^{-3}\text{h}^{-1}$$

where $r_i$ is the number of observed failures, $T_{\Sigma,i}$ is the total accumulated operating time

Which gives (27):

$$MTBF_1 = \frac{1}{\lambda_1} = \frac{1}{1.50 \times 10^{-3}} = 666.67h$$

Applying the same relationships to the remaining loading regimes produced: $\lambda_2=2.50\times10^{-3}$ h$^{-1}$,$MTBF_2$ =400.00 h, and $\lambda_3=3.50\times10^{-3}$ h$^{-1}$,$MTBF_3$=285.71 h. Thus - $\lambda1<\lambda2<\lambda3$.

The variable-overload regime produced a failure rate approximately 1.67 times higher than that obtained under symmetric loading, whereas the asymmetric-loading regime increased the failure rate by a factor of approximately 2.33.

Accordingly, intermittent overloads reduced the MTBF by 40.00%, while the combined influence of increased radial loading and shaft eccentricity reduced it by 57.14% relative to the symmetric-loading scenario.

The calculated failure rates and mean operating times indicate that the deterioration of reliability is not governed only by the nominal torque. Although the nominal torque and rotational speed remained unchanged, the introduction of intermittent overloads increased the number of failures from three to five. A further increase to seven failures was obtained under asymmetric loading. This result demonstrates the considerable influence of radial-force imbalance and eccentricity on the operational reliability of the shaft–bearing assembly.

Using Equation (8), the probabilities of failure-free operation were calculated for operating times of 100, 250, and 500 h.

$$P(t) = e^{-\lambda_1 t}; \;\; \lambda_1(t) = const$$

$$P_1(t) = exp(-\lambda_1 t) = P_1(100) = exp(-0.0015.100) = 0.860$$

The probability of failure *Q(t)* (10):

$$Q_1(100) = 1 - P_1(100) = 1 - 0.8607 = 0.1393$$

The failure probability densities (13).

$$f_1(t) = \lambda_1(t)P_1(t) = 1.50 \times 10^{-3} \times 0.8607 = 1.2911 \times 10$$

The calculated values are presented in Table 5.

After 100 h, the probability of failure-free operation decreased from 0.8607 under symmetric loading to 0.7788 under variable loading and to 0.7047 under asymmetric loading. The differences became more pronounced as the operating time increased. At 500 h, the respective reliability probabilities were 0.4724, 0.2865, and 0.1738.

The calculated probabilities of failure-free operation for the three loading scenarios are presented in Figure 6.

As shown in Figure 6, the symmetric constant-loading scenario maintains the highest probability of failure-free operation throughout the investigated time interval. The asymmetric loading scenario exhibits the most rapid reliability degradation, while the variable-overload scenario shows intermediate behaviour.

*Table 5. Time-dependent reliability indicators for the investigated loading scenarios*

| Loading scenario | Operating time t, h | P(t) | Q(t) | f(t), h⁻¹ |
|---|---|---|---|---|
| Symmetric constant loading | 100 | 0.861 | 0.14 | $1.29\times10^{-3}$ |
| | 250 | 0.687 | 0.313 | $1.03\times10^{-3}$ |
| | 500 | 0.472 | 0.528 | $7.09\times10^{-4}$ |
| Variable loading with IO | 100 | 0.779 | 0.221 | $1.95\times10^{-3}$ |
| | 250 | 0.535 | 0.464 | $1.33\times10^{-3}$ |
| | 500 | 0.287 | 0.714 | $7.16\times10^{-4}$ |
| Asymmetr. constant loading | 100 | 0.705 | 0.295 | $2.46\times10^{-3}$ |
| | 250 | 0.417 | 0.583 | $1.45\times10^{-3}$ |
| | 500 | 0.175 | 0.826 | $6.08\times10^{-4}$ |

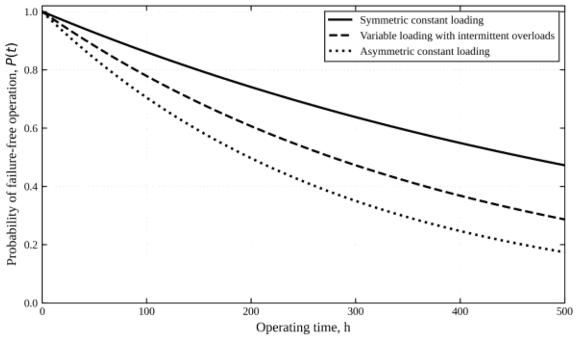


*Figure 6: Probability of failure-free operation under different loading conditions.*

After 100 h, the probability of failure-free operation decreased from 0.8607 under symmetric loading to 0.7788 under variable loading and to 0.7047 under asymmetric loading. The differences became more pronounced with increasing operating time. At 500 h, the corresponding reliability probabilities were 0.4724, 0.2865, and 0.1738, respectively.

Although the failure rate $\lambda_i$ remains constant within each adopted exponential model, the failure probability density $f_i(t)$ decreases with operating time because it also depends on the probability that the assembly has survived without failure up to time $t$. Therefore, the lower value of $f(t)$ obtained for the asymmetric regime at 500 h must not be interpreted as improved reliability. It results from the substantially smaller surviving population associated with this loading regime.

The corresponding failure probability density functions are illustrated in Figure 7.

Figure 7 shows that the failure probability density decreases with operating time for all three scenarios. The initially higher values associated with the more severe loading regimes reflect their higher failure rates. The subsequent decrease does not indicate improved reliability, but results from the progressively smaller proportion of assemblies remaining operational without failure.

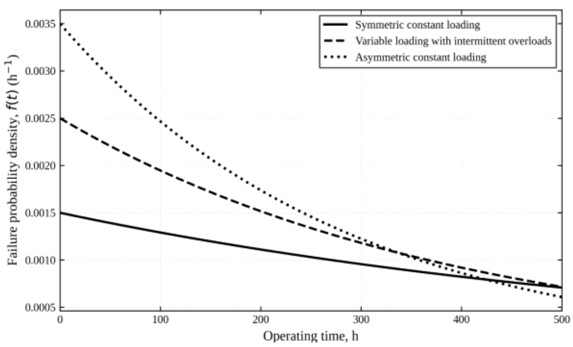


*Figure 7: Failure probability density under different loading conditions.*

To provide a general representation of the combined influence of operating time and failure rate, the reliability assessment space is presented in Fig. 8.

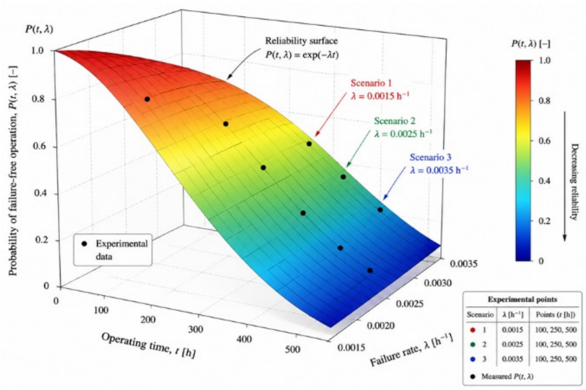


*Figure 8: Three-dimensional reliability assessment space.*

Figure 8 confirms the combined effect of operating time and failure rate on shaft reliability. Reliability decreases monotonically with both increasing operating time and increasing failure rate. The three investigated scenarios occupy distinct regions of the reliability surface, with the asymmetric loading regime consistently corresponding to the lowest probability of failure-free operation.

According to Equation (26), the mean restoration times were:

$$MTTR = \frac{1}{n}\sum_{i=1}^{n} T_{Ri} \rightarrow MTTR_1 = \frac{T_{R1}}{r_1} = \frac{18}{3} = 6.00h$$

and the corresponding restoration rate was (33)

$$\mu_1 = \frac{1}{MTTR_1} = \frac{1}{6.00} = 0.1667\ h^{-1}$$

The stationary availability coefficient was therefore (34):

$$K_{A1} = \frac{MTBF_1}{MTBF_1 + MTTR_1} = \frac{666.67}{666.67 + 6} = 0.9911$$

Applying the same procedure to the variable-overload and asymmetric-loading regimes gave: $MTTR_2 = MTTR_3 = 7.00$ h, $\mu_2 = \mu_3 = 0.1429\ h^{-1}$, and $K_{A,2} = 0.9828$, $K_{A,3} = 0.9761$.

The calculated reliability and maintainability indicators are summarised in Table 6.

*Table 6. Time-dependent reliability indicators for the investigated loading scenarios*

| Sc. | λ, h⁻¹ | MTBF | MTTR | μ, h⁻¹ | $K_A$ |
|---|---|---|---|---|---|
| 1 | $1.50\times10^{-3}$ | 666.67 | 6.00 | 0.1667 | 0.991 |
| 2 | $2.50\times10^{-3}$ | 400.00 | 7.00 | 0.1429 | 0.983 |
| 3 | $3.50\times10^{-3}$ | 285.71 | 7.00 | 0.1429 | 0.976 |

The availability remained relatively high in all three cases because the restoration time was considerably shorter than the mean operating time between successive failures. Nevertheless, the reduction from 0.9911 to 0.9761 represents a meaningful deterioration for continuously operating industrial equipment. Even a comparatively small reduction in availability may lead to additional downtime, interrupted production cycles, and increased maintenance costs over a large number of operating cycles.

From a practical perspective, the obtained reliability indicators provide a quantitative basis for comparing the investigated dynamic loading configurations and identifying operating conditions associated with increased mechanical loading and reduced reliability. The results can support the selection of appropriate operating regimes of the experimental test rig, the identification of potentially critical loading configurations, and the planning of inspection and maintenance activities. The proposed assessment can also be applied to similar laboratory shaft–bearing systems operating under cyclic dynamic loading.

## 5. Conclusions

This study presented a dynamic reliability assessment of a rotating shaft subjected to operational loading conditions using an exponential reliability model with a constant failure rate. The proposed methodology combines classical reliability theory with engineering performance indicators, providing a practical framework for evaluating the operational reliability and availability of rotating mechanical components.

The main conclusions can be summarized as follows:

1. A mathematical reliability model based on the exponential lifetime distribution was successfully developed for three representative operating scenarios characterized by different failure rates. The model enables direct prediction of the probability of failure-free operation over the considered service interval.
2. The influence of the failure rate on system reliability was quantitatively evaluated. An increase in the failure rate from 0.0015 $h^{-1}$ to 0.0035 $h^{-1}$ resulted in a significant reduction in the probability of reliable operation, confirming the strong sensitivity of reliability to deterioration of operating conditions.
3. The calculated MTBF, MTTR, and availability values provide complementary indicators for maintenance planning and operational decision-making. Although availability remained above 97 % for all investigated scenarios, the reliability decreased considerably with increasing operating time and failure rate.
4. The reliability curves obtained for the three loading scenarios clearly demonstrate the progressive reduction in system reliability with service time, allowing the identification of operating periods in which preventive maintenance should be considered before a significant decrease in reliability occurs.
5. The proposed methodology is computationally efficient, requires only a limited number of engineering reliability parameters, and can be readily implemented during the design, assessment, or maintenance planning of rotating shafts and similar mechanical components.
6. Although the present investigation is based on the assumption of a constant failure rate, the developed methodology establishes a solid foundation for future extensions involving variable failure-rate models, experimental validation, and probabilistic lifetime distributions applicable to more complex degradation processes.

Overall, the presented approach offers a simple, robust, and practically applicable engineering tool for reliability assessment of rotating mechanical systems and may support reliability-based design, maintenance optimization, and lifecycle management in industrial applications.

Future research will focus on the integration of experimentally identified degradation mechanisms, advanced probabilistic lifetime models, and condition-based monitoring techniques in order to further improve the predictive capability and engineering applicability of the proposed reliability assessment methodology.

## Acknowledgement

The authors would like to thank the Research and Development Sector at the Technical University of Sofia for the financial support.

## References

[1] Friswell, M. I., *Dynamics of Rotating Machines,* Cambridge University Press, Cambridge, UK, 2010. *https://doi.org/10.1017/CBO9780511780509*
[2] Vance, J. M., Zeidan, F. Y., and Murphy, B., *Machinery Vibration and Rotordynamics*, John Wiley & Sons, Hoboken, NJ, USA, 2010. *https://doi.org/10.1002/9780470903704.index*
[3] Ehrich, F. F., *Handbook of Rotordynamics*, McGraw-Hill, New York, NY, USA, 1992. ISBN : 9781575240886
[4] Rao, J. S., *Rotor Dynamics*, 3rd ed., New Age International Publishers, New Delhi, India, 1996.
[5] Muszynska, A., *Rotordynamics*, CRC Press, Boca Raton, FL, USA, 2005.
[6] Darpe, A. K., Gupta, K., and Chawla, A., Coupled Bending, Longitudinal and Torsional Vibrations

of a Cracked Rotor, *Journal of Sound and Vibration*, vol. 269, no. 1–2, pp. 33–60, 2004. *DOI:10.1016/S0022-460X(03)00003-8*

[7] Patel, T. H., and Darpe, A. K., Coupled Bending–Torsional Vibration Analysis of a Rotor with Rub and Crack Faults, *Journal of Sound and Vibration*, vol. 326, no. 3–5, pp. 740–752, 2009. *DOI:10.1016/j.jsv.2009.05.020*

[8] Al-Bedoor, B. O., Modeling the Coupled Torsional and Lateral Vibrations of Unbalanced Rotor Systems, *Computer Methods in Applied Mechanics and Engineering*, vol. 190, pp. 5999–6008, 2001. *DOI:10.1016/S0045-7825(01)00209-2*

[9] Rao, M. A., Srinivas, J., Rama Raju, V. B. V., and Kumar, K. V. S. S., Coupled Torsional–Lateral Vibration Analysis of Geared Shaft Systems, *Journal of Sound and Vibration*, vol. 261, no. 2, pp. 359–364, 2003. *DOI:10.1016/S0022-460X(02)01240-3*

[10] Li, L., Ma, T., Liang, F., & Xie, F. (2025). Nonlinear Dynamic Modeling of Rotor-Bearing Systems with Combined Support Considering Coupled Motion: Numerical and Experimental Studies. *Mathematics*, *13* (22), 3694. *https://doi.org/10.3390/math13223694*
Shi, C., Ma, Y., Wang, Y., Chen, X., and Hong, J., Frequency Modulation of Coupled Lateral–Torsional Vibrations in Rotor Systems, *Journal of Sound and Vibration*, vol. 611, Article 119157, 2025. *DOI:10.1016/j.jsv.2025.119157*

[11] Petrov, N., Dimitrov, V., and Dimitrova, V., *Reliability of Technology Systems in Industrial Manufacturing*, AkiNik Publications, New Delhi, India, 2018.

[12] ISO 20816-1:2016, *Mechanical Vibration—Measurement and Evaluation of Machine Vibration—Part 1: General Guidelines*, International Organization for Standardization, Geneva, Switzerland, 2016.

[13] ISO 21940-11:2016, *Mechanical Vibration—Rotor Balancing—Part 11: Procedures and Tolerances for Rotors with Rigid Behaviour*, International Organization for Standardization, Geneva, Switzerland, 2016.

[14] Tonkova, G., Nikolov, N. N., Experimental Study of Bending and Torsional Vibrations of Shafts, *International Virtual Journal for Science, Technics and Innovations for the Industry Machines*, Technologies, Materials, Year IV, No. 1–2, pp. 11–16, 2010.

[15] Valkov, M. V., and Tonkova, G., Load-Carrying Capacity Assessment of a Shaft in an Experimental Test Rig, *Proceedings of the XV International Scientific Conference VSU'2015*, Vol. II, pp. 71–76, 2015 (in Bulgarian).

[16] Tonkova, G., Trifonova-Genova, V., Determining the Natural Frequency of a Stepped Shaft with a Transitional Curved Section, *Journal of Mining and Geological Sciences "St. Ivan Rilski"*, Vol. 61, Part III, pp. 60–63, 2018.

[17] Tonkov G., M. Teofilova, G. Tonkova. Software and management in CAD technologies of production systems and related information-management processes. Journal of International Scientific Publication: Economy & Business, Volume 3, Part 1, 2009, (page 582-590), ISSN 1313-2555.

[18] Tonkova G. Z., *Investigation of the Influence of Bending and Torsional Vibrations of Shafts Used in Heavy Mining Machinery*, Ph.D. dissertation, Dept. of Mine Mechanization, Faculty of Mining Electromechanics, University of Mining and Geology "St. Ivan Rilski", Sofia, Bulgaria, 2017.